

GEOCHEMISTRY OF MANGANESE- IRON ORES AT UM BOGMA AREA, WEST CENTRAL SINAI, EGYPT

Ibrahim H. Khalifa & Rehab A. Seif

Geology Department, Faculty of science, Suez Canal University, Ismailia, Egypt
Ibrahim_kh_2000@yahoo.com

ABSTRACT

The Um Bogma manganese-iron deposit occurs within different levels of the Lower and Middle Members of Um Bogma Formation of Paleozoic age. The mineralization was observed lenticular, banded, pockets and encrustation forms. The geochemical characteristics of the Um Bogma deposit was studied by means of major oxide, trace element contents and the origin of mineralization was discussed. Three types of Mn-Fe ores were identified based on field occurrences, MnO and Fe₂O₃ contents and MnO/Fe₂O₃ ratios: (1) Mn-rich ore; (2) Fe-Mn rich ore and (3) Fe-rich ore. The correlation coefficients indicated the presence of strong negative correlation coefficient between MnO and Fe₂O₃ ($r=-0.94$) reflects the precipitation of manganese and iron under different environmental conditions. Ba and Cu show positive correlation coefficients with MnO ($r= 0.75$ and $r= 0.63$ respectively) and negative correlation with Fe₂O₃ ($r= -0.60$ and $r= -0.56$ respectively) suggest their selective adsorption on manganese oxides. The positive correlation coefficients between the trace elements; Co-Ni ($r= 0.66$), Co-Cu ($r=0.80$), Co-Zn ($r=0.57$), Ni-Zn ($r=0.80$), Cu-Zn ($r= 0.57$), Cu-Pb ($r= 0.80$) Zn-Pb ($r=0.51$) indicate their precipitation from hydrothermal solutions. The discrimination diagrams based on major and trace elements, the high Mn/Fe ratios, the low Co/Zn, the high contents of Cu, Pb, Zn and Ni and the low contents of Al and Ti indicated that the Um Bogma manganese deposit is a hydrothermal-type mineralization.

Keyword: Geochemistry, Manganese-iron ores, Um Bogma, Sinai

1. INTRODUCTION

Manganese ore deposits occur in a great diversity of host rocks such as carbonate, siliciclastic, volcanic and metamorphic rocks and range in ages throughout geologic history. Marine manganese oxide deposits are classified based on their mineralogy, composition and tectonic settings as hydrogenous, diagenetic and hydrothermal deposits (Hein et al., 1997). Hydrogenous manganese deposits are those slowly precipitated from seawater (Ingram, et al., 1990) and composed of amorphous iron and are poor in manganese oxide. The Mn/Fe ratio is ~1 and Ni and Cu are represented by high concentrations (>3000 ppm). Diagenetic manganese deposits occur as nodules and are precipitated from hydrothermal solutions or pore waters within altered sediments (Klinkhammer et al., 1982 and Manheim et al., 1988). Hydrothermal manganese oxide deposits are directly precipitated from low-temperature hydrothermal solutions in continental environments or sedimentary exhalative manganese mineralization deposited in marine environments (Ingram, et al.; 1990, Nicholson; 1992a and Hein et al.; 1997). These deposits are generally of laminated and stratabound forms. Diagenetic and hydrothermal deposits are characterized by high Mn/Fe ratios (Hein et al., 1994 and 1996). Although there are some similarities between these two deposit types, they are mostly distinguished with their morphologic, tectonic and growth rates (Kuhn et al., 1998).

The Um Bogma manganese-iron deposit is a large stratiform manganese-iron oxide orebody contained in carbonate rocks of marine origin. It is reported since 1907 by Barron in the Paleozoic sediments which consist of sandstones, shales, sandy shales and dolomites, however, manganese have been exploited in the period starting from 1918 up to the present. The origin of Um Bogma manganese deposits is still a matter of controversy, where some authors considered the manganese ore is of sedimentary origin (El-Shazly et al.; 1963, Kotchin et al., 1968, Mart

and Saas; 1972, Saleeb-Roufaiel et al.; 1987, Kora; 1994, El Agami; 1996). Other authors believed that they are of hydrothermal origin (Ball; 1916, Attia; 1956, Gill and Ford; 1956, Nakhla and Shehata; 1963, Basta and Saleeb; 1971, Saad et al., 1994) or even of supergene origin (El-Sharkawy et al. 1990). In the present study, the geological setting and major and trace element contents of the mineralization were determined and then these data were used for determination of formation conditions of mineralization.

2. REGIONAL GEOLOGY

Manganese-iron ores are frequently distributed with different proportion, thickness, length and forms within the Paleozoic sediments in the Um Bogma area. The most important and economic occurrences of Mn-Fe ores were located within Um Bogma Formation. Generally they are occurring in different levels as layers, sheets, lenses and pockets in the Lower and Middle Members of Um Bogma Formation. The ores consist of a heterogeneous mixture in varying proportions of iron and manganese oxides.

The Paleozoic sequence at the study area is unconformably overlies the Precambrian basement rocks and underlies the Triassic basaltic sheets (Figures 1 & 2a). It attains a thickness ranges from 160 to 365m (El Fiky, 1988) and divided into Lower Sandstones Series, Middle Carboniferous Limestone Series and Upper Sandstones Series (Barron, 1907). The Lower Sandstone Series (~ 130m thick) belong to the Cambro-Ordovician age (Issawi and Jux, 1982), overlies unconformably a flat, weathered plain surface of the crystalline basement rocks. They consist of alternating sequence of sandstone and shales. Impregnations of manganese minerals are common in its lower part, while some copper mineralization appears in its upper part. They

comprise Sarabit El Khadim, Abu Hamata, and Adedia Formations (Soliman and Abu El Fetouh, 1969).

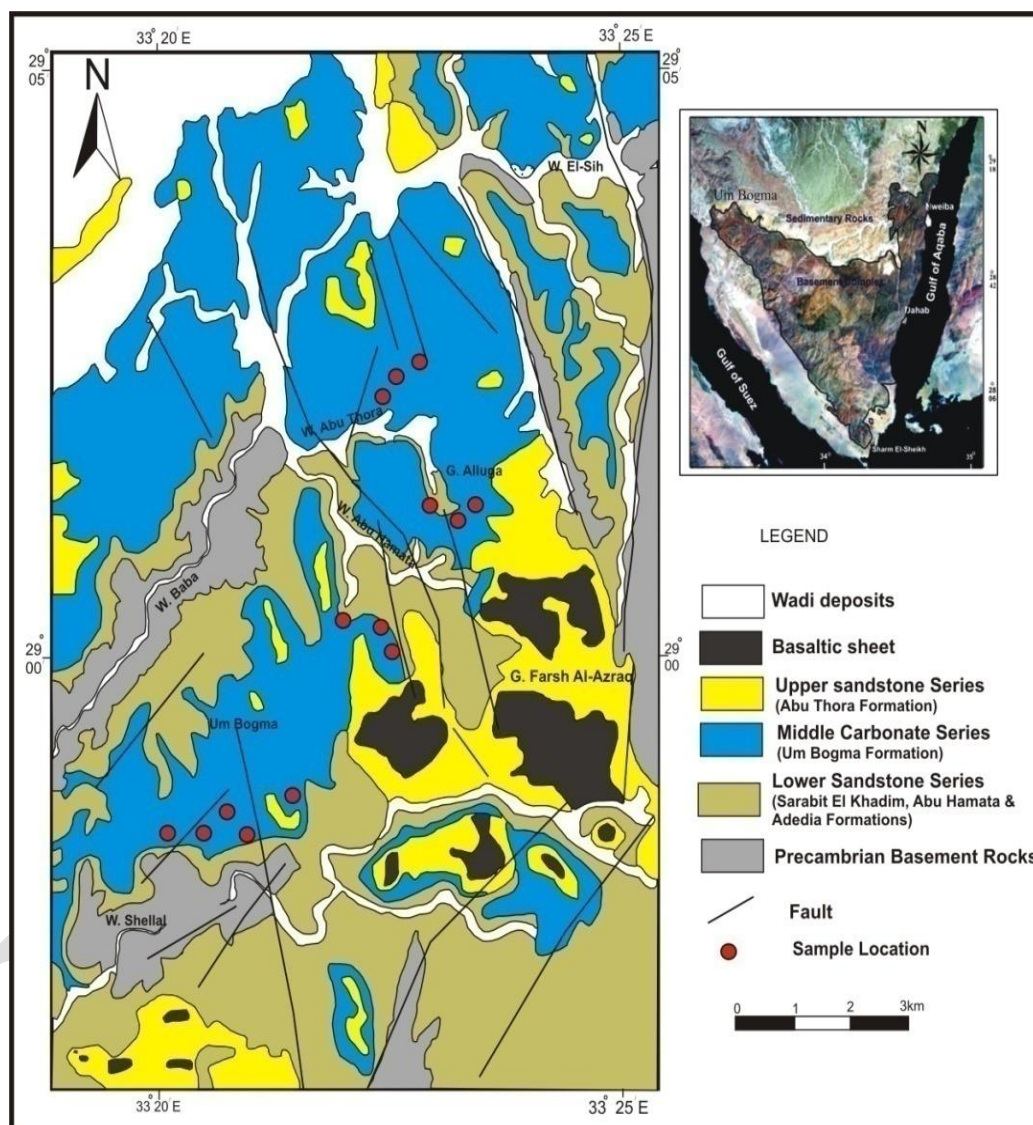


Figure 1: Geologic map of Um Bogma area.

Sarabit El Khadim Formation (16-20m thick) starts from its base by compact gravely sandstone interbedded with muddy brownish sandstone which graded upward to fine-grained brownish and friable sandstone followed by brownish laminated, fine-grained sandstone containing thin lenses of conglomerate and finally white gravely sandstone.

Abu Hamata Formation (40-62m thick) are fine-laminated, thin bedded, yellowish white to grey, fine-grained sandstone containing green copper carbonate staining as well as spots, patches and encrustations of manganese oxides. This sequence is graded upward to grey, fine laminated and fissile shaly sandstone containing some green staining of copper carbonate minerals along their fissile planes. The upper boundary is characterized by change from the shale to sandstone.

Adedia Formation is conformably consists of sandstone and siltstone. They are fine-grained with varying color from white to yellow, massive, cross-laminated, and showing many sedimentary structures such as tabular planar and trough cross-bedding. The thickness of Adedia Formation ranges from 30 meters at Gebel Alluga to 60 meters at Wadi Abu Hamata.

The Middle Carboniferous Series is known as Um Bogma Formation (Weissbrod, 1981), overlies unconformably Adedia Formation (Figure 2c) and also unconformable overlain by Abu Thora Formation. They are of a Tournasian-Visean age (Kora and Jux 1986; Kora, 1989) and consist of hard crystalline dolomite with some limestone and marl layers. Their thickness changes from 6m to about 40m with tendency of gradual decrease in thickness towards the southeast (at the center of the studied area) reflecting a gradual shallowing of the Carboniferous sea in this direction (Kora et al., 1994). This Formation is considered as a polymetallic rock unit due their association with iron and manganese oxides, and secondary copper mineralization. This formation was subdivided into three members by several workers (Weissbrod; 1969, Kora; 1984, El Sharkawi et al.; 1990, Mansour; 1994, Kora et al.; 1994, and Ashami; 2003). The basal unit of Um Bogma Formation is unconformably overlain the sandstone of Adedia Formation (Figure 2c). The thickness of this member differs from place to another but its maximum section (17 meter) was measured by Kora (1989) at the entrance of Wadi Baba. It is composed of hard,

thickly bedded, pink-brown and coarsely crystalline dolomite containing manganese-iron concretions and lenses as well as secondary copper minerals filling the fracture. The Middle marly dolomite Member is composed of intercalations of yellowish marl and brown very hard massive marly dolomite and dolomitic limestone (Figure 2d). The Upper member rests conformably over the middle marly dolomite.

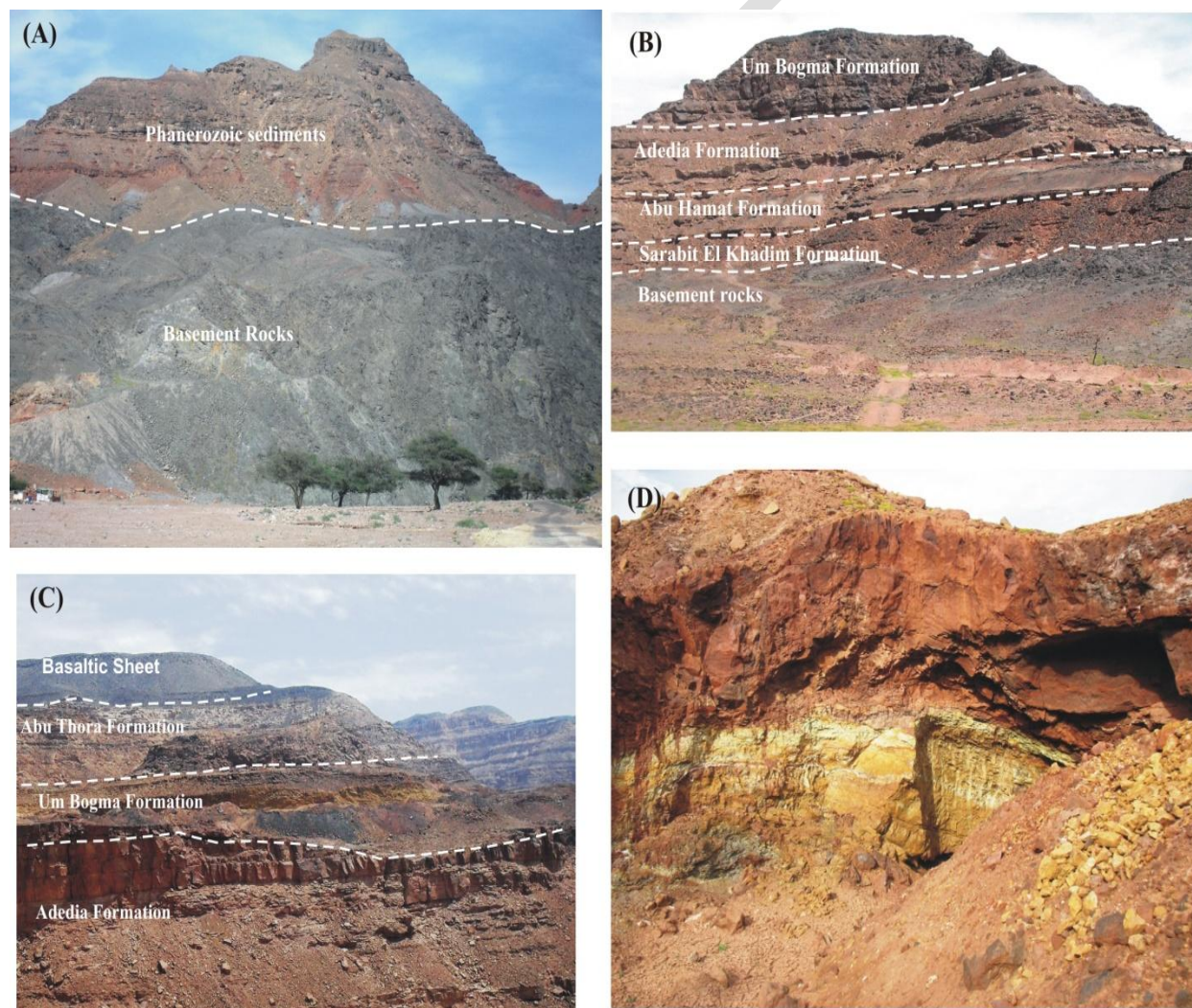


Figure 2: Photographs showing (A) The basement rocks at the entrance of Wadi Baba, unconformably overlain by the Paleozoic rocks, (B) General view of Paleozoic sediments at Gabal Alluga, (C) Um Bogma Formation unconformably overlies the Adedia Formation at Wadi Abu Hamata, (D) The pink dolomite of Upper Dolomite member conformably overlain the marly dolomite of Middle Carbonate Member, Um Bogma Formation at Wadi Abu Hamata.

The Upper Sandstone Series is known as Abu Thora Formation (Kora, 1984). It was subdivided into three formations by Soliman and Abu El Fetouh (1969) from base to top; El Hashash, Magharet El Maiah and Abu Zarab. This series are composed of shale, siltstone, sandstone, kaolin, clay and carbonaceous shale. They show lateral variations in lithology, where the kaolin and clay beds change laterally into carbonaceous shale. It varies in thickness from locality to other, it attain a thickness of 33 meter at Gebel Alluga and 60 meter at Wadi Abu Hamata and Shellal localities. Basaltic sheets are usually overlies the Paleozoic section at the top of Gebel Farsh El Azraq and at the entrance of Wadi Shellal (Figure 1). It is about 60m in thickness (Hussein et al, 1971) and of probable Triassic age (Weissbrod, 1969).

3. FIELD OCCURRENCE

The manganese- iron ores are located as a series of disconnected lenses (2.0 to 3.0 m thick) in the lower part of the Dolostone Member that overlies the unconformity surface separating the Adedia Formation from Um Bogma Formation (Figures 3a & 3b). Manganese mineralization is also observed filling the open spaces and vugs in the dolomite rocks of the Dolostone (Figure 3c & 3d). In many occurrences, the manganese lenses are completely separated from the iron ore or occasionally, they were surrounded by iron ores or changed vertically into more iron-rich ores.

Manganese-iron deposits are also recorded in several levels within the Marly dolomite and siltstone Member of Um Bogma Formation. Many excavated mines are opened along the middle member of Um Bogma Formation at Wadi Shellal (Figure 3e). The manganese lenses are about 2 to 3 meter thick and enclosed within varicolored layers of shale, marl and dolomite. The ore in many localities appear as alternating sheets of manganese and iron oxides parallel to the

bedding planes (Figure 3 f). Green copper mineralization is detected along the fissile planes of marl of the Marly dolomite Member of Um Bogma Formation overlying the manganese ores.

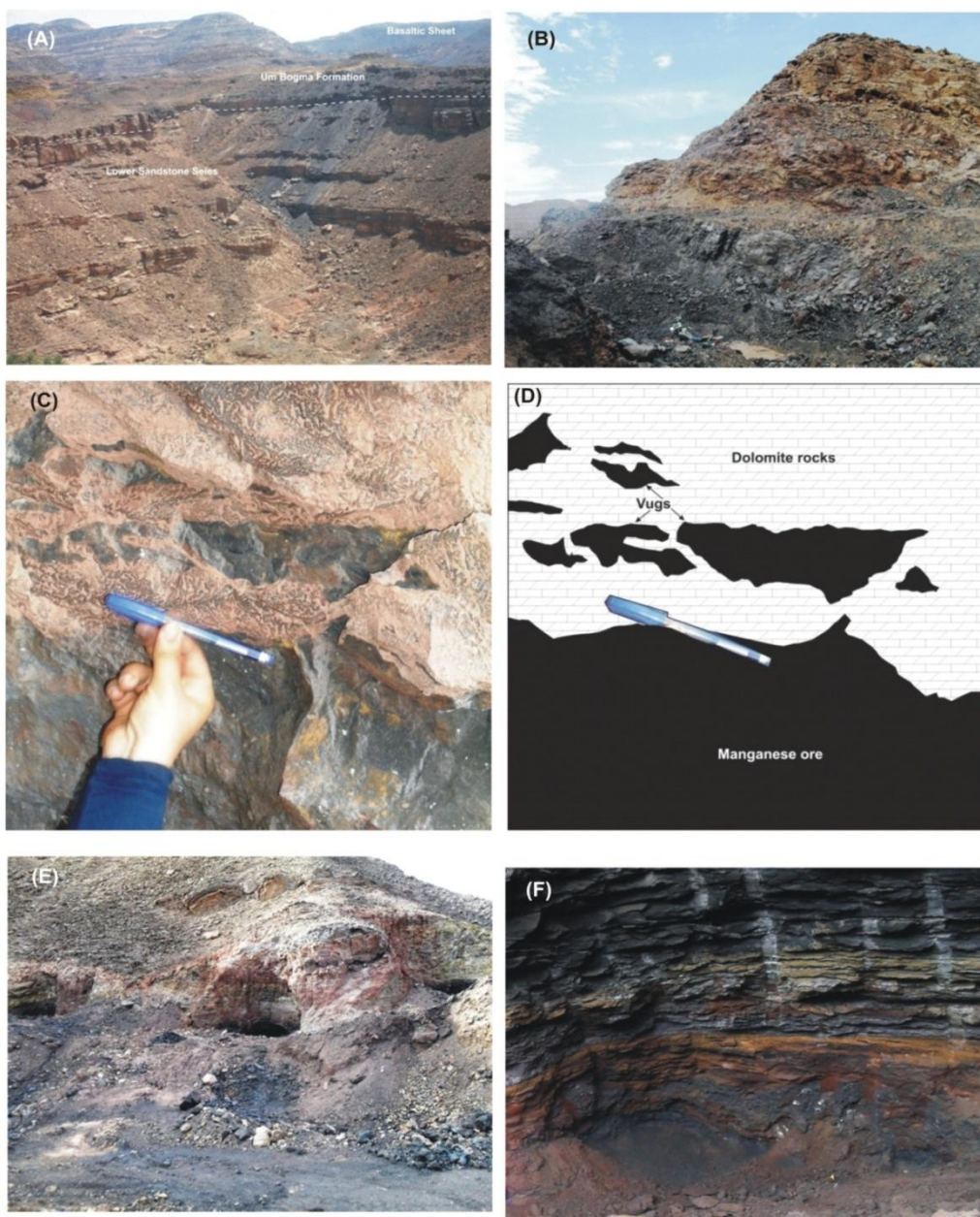


Figure 3: Photographs showing (A) Manganese ore at the base of the Lower Member of Um Bogma Formation, Wadi Abu Thora area, (B) Excavated manganese lens between the Lower and the Middle Dolomite Members at Wadi Abu Hamata area, (C) Open space and vugs filled with manganese ore within the Lower dolomite Member of Um Bogma Formation at Wadi Shellal, (D) Sketch illustrate figure c, (E) excavated mines of manganese ore in the Middle dolomite Member of Um Bogma Formation, Wadi Shellal, (F) Alternating sheets of iron oxides and manganese oxide in the Middle dolomite Member of Um Bogma Formation.

4. GEOCHEMISTRY

4.1. Materials and Method

The materials of this study are 14 Mn-Fe ore samples of which 3 samples were collected from Abu Thora, 3 samples from Abu Hamata, 3 samples from Alluga and 5 samples from Shellal localities (Fig.1). Major and trace element contents of these samples were determined using X-ray Fluorescence Spectrometry at the Central Laboratories of Egyptian Mineral Resources Authority (EMRA). The compositions of manganese ore were determined using X-ray diffraction techniques at the X-ray laboratory of Geology Department, Suez Canal University. Correlation coefficient techniques are used to assess in making geochemical inference on the origin of Fe-Mn ores at Um Bogma area using SPSS software.

4.2. MINERALOGY

Due to the similarity of the X-ray diffraction patterns of the eight samples that carried out during the present study, only two patterns are presented here. The X-Ray diffraction patterns of the Mn-rich samples confirmed the presence of pyrolusite and amorphous Mn oxides on the XRD spectrum. The position of lowest and highest peak of pyrolusite is shown in figure (Figure 4).

4.3. Geochemical Classification

The iron-manganese deposits in the study area are chemically classified into three types depending on their MnO and Fe₂O₃ contents and the MnO/Fe₂O₃ ratios (Table 1).

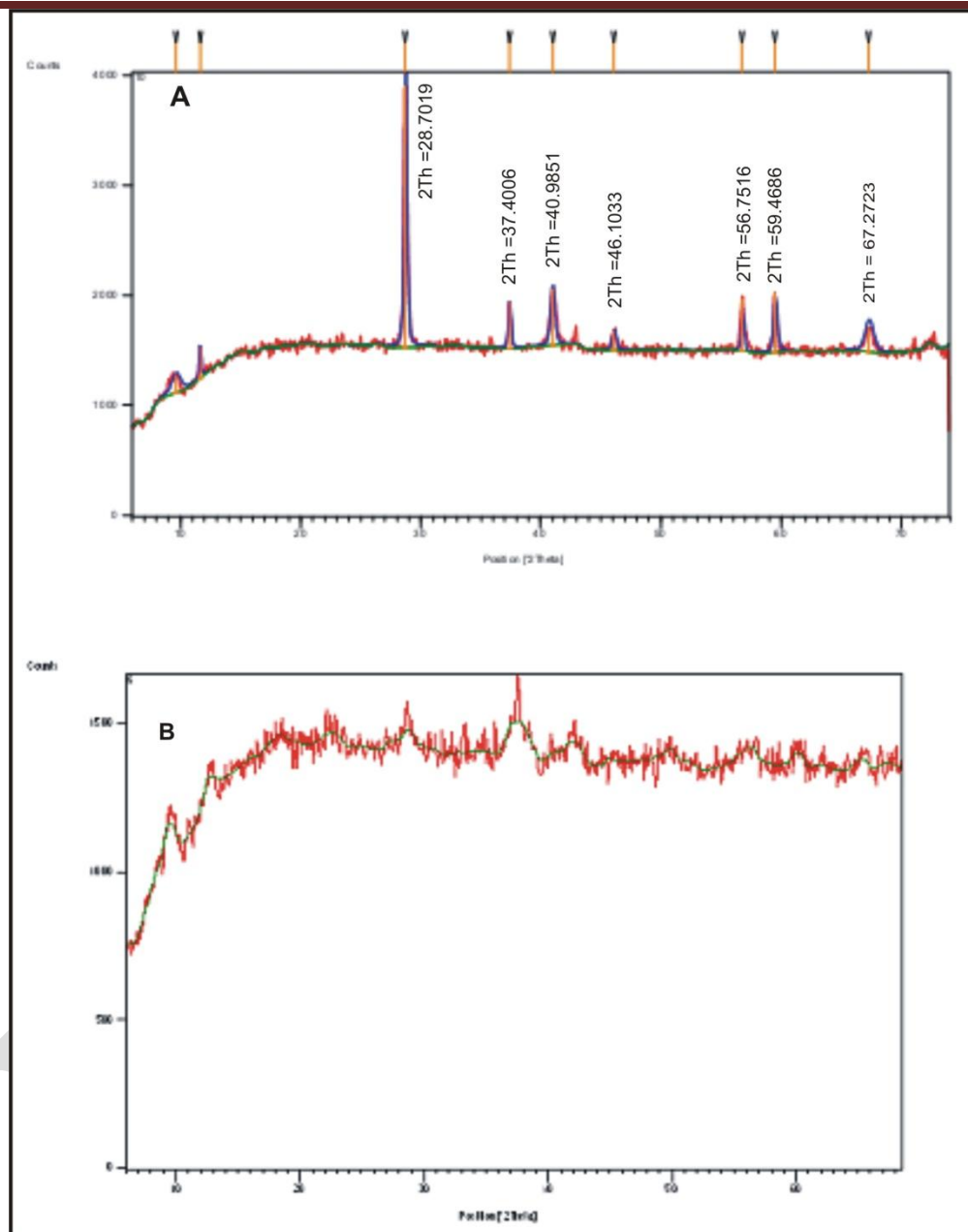


Figure 4: X-ray diffraction pattern of (A) crystalline Mn-rich ore (sample no.10) and (B) amorphous Mn-rich ore (sample no.6), Um Bogma area.

4.3.1. Type 1: Mn-rich ore type

Mn-rich ore exposed mainly at Gabal Alluga and El Shellal localities. It is characterized by high MnO contents range between 71.88 to 82.56 wt % (average 78.51 wt %) and Fe_2O_3 contents range between 1.02 to 5.04 wt % (average 2.46 wt %) with MnO/ Fe_2O_3 ratios range

between 14.26 to 80.94 (average 45.09). This type is characterized by low contents of SiO_2 (0.88 to 2.90 wt %, average 1.57 wt %), TiO_2 (average 0.05 wt %), V (average 207ppm), Sr (average 661 ppm) and Nb contents (average 1.5ppm). Conversely, this type is characterized by relatively high contents of Al_2O_3 (average 1.32 wt %), Cu (average 2268ppm), Zn (average 1471), Co (average 185ppm), Pb (average 147ppm), Ni (average 161ppm), Ba (average 2435ppm) and Zr (average 119ppm). The high contents of Cu, Zn, Pb, Ni and Ba may be due to their adsorption into manganese oxides.

4.3.2. Type 2- Mn-Fe rich ore

Mn-Fe-rich ore occurs mainly at Abu Hamata and El Shellal localities. It is characterized by more or less equal contents of both MnO and Fe_2O_3 . The MnO contents range between 26.80 to 44.90 wt % (average 36.01 wt %) and Fe_2O_3 contents range between 13.19 to 53.70 wt % (average 36.55%) with an MnO/ Fe_2O_3 ratios range between 0.5 to 3.15 (average 1.46). This type is relatively enriched with SO_3 (average 1.28%), Zn (average 951ppm), Sr (average 687) and depleted with Al_2O_3 (average 0.55%), TiO_2 (0.05%), Co (79), Ni (105ppm) and Cu (8ppm). On the other hand, they have intermediate compositions of SiO_2 (average 2.05%), Cr (average 375ppm), V (average 312ppm) and Zr (77ppm) between the other two types.

4.3.3. Type 3 Fe-rich ore type

Fe-rich ore occurs at Gabal Abu Thora and Gabal Abu Hamata localities where the ore lenses are composed mostly of Fe-oxides with Fe_2O_3 contents range between 80.90 to 90.5 wt % (average 84.99 wt %) and MnO contents range between 0.18 to 6.20 wt % (average 1.33 wt%) with an MnO/ Fe_2O_3 ratios range between 0.0 to 0.07 (average 0.02). This type is also

characterized by low contents of Al_2O_3 (average 0.51 wt %), SO_3 (average 0.01 wt%), Cu (88ppm), Sr (average 358ppm), Ba (average 142ppm), Pb (average 71ppm) and Zr (average 82ppm). On the other hand, it is characterized by relatively high contents of SiO_2 range between 4.60 to 10.10 wt % (average 7.62 wt %), TiO_2 (average 0.48 wt %), V (average 569ppm), Cr (average 935ppm) Co (average 247ppm), Ni (average 312ppm), Zn (average 836ppm), and Nb (average 6ppm). The high concentration V, Ni, Co and Cr in this type of ore is possibly due to the adsorption these elements on the hydrous Fe-oxides.

5. DISCUSSIONS

5.1 Correlation Coefficients

The correlations among major and trace element concentrations of ore samples at Um Bogma area are illustrated in Table (2). The strong negative correlation coefficient between MnO and Fe_2O_3 ($r=-0.94$) suggests their precipitation under different environmental conditions where the fractionation between these two elements takes place during their formation (Krauskopf, 1957). Even though, Fe and Mn have very similar behavior, Mn has more mobility than Fe especially in sedimentary environments (Simmonds and Ghasemi, 2007). Accordingly Fe precipitates sooner than Mn, so that they are differentiated and segregated from each other. . Ba and Cu show positive correlation coefficients with MnO ($r= 0.75$ and $r= 0.63$ respectively) and negative correlation with Fe_2O_3 ($r=-0.60$ and $r= -0.56$ respectively) which reflects their selective adsorption on the manganese oxides rather than iron oxides. This may explain the derivation of manganese from a hydrothermal source where hydrothermal solutions are more enriched in Ba and Cu compared to seawater since they are affected from volcanic activity and sedimentation (Monnin et al., 2001).

Table 1: Major oxides and trace elements contents in the Um Bogma Mn-Fe ores.

| Sample | 1 | 2 | 3 | 4 | 5 | 6 | 7 | 8 | 9 | 10 | 11 | 12 | 13 | 14 |
|--|-----------|-------|-------|-----------|-------|-------|------------|-------|-------|---------|-------|-------|-------|-------|
| locality | Abu Thora | | | Al-Alluga | | | Abu Hamata | | | Shellal | | | | |
| Major oxides in % | | | | | | | | | | | | | | |
| SiO ₂ | 9.80 | 8.60 | 10.10 | 0.88 | 1.07 | 2.90 | 7.20 | 5.40 | 1.31 | 1.43 | 1.52 | 2.90 | 2.46 | 4.60 |
| TiO ₂ | 0.75 | 0.70 | 0.76 | 0.02 | 0.02 | 0.13 | 0.24 | 0.28 | 0.04 | 0.03 | 0.02 | 0.09 | 0.03 | 0.15 |
| Al ₂ O ₃ | 1.04 | 0.37 | 1.25 | 0.45 | 1.24 | 3.16 | 0.20 | 0.21 | 0.40 | 0.43 | 0.26 | 0.69 | 0.84 | 0.00 |
| Fe ₂ O ₃ | 82.70 | 85.60 | 80.90 | 1.02 | 2.09 | 5.04 | 87.20 | 90.50 | 13.19 | 1.70 | 28.60 | 50.70 | 53.70 | 83.03 |
| MnO | 0.18 | 0.25 | 0.41 | 82.56 | 79.50 | 71.88 | 0.53 | 0.38 | 41.50 | 80.10 | 44.90 | 30.85 | 26.80 | 6.20 |
| MgO | 0.84 | 0.52 | 1.22 | 0.30 | 0.39 | 0.17 | 0.65 | 0.81 | 1.82 | 0.44 | 0.86 | 0.88 | 0.83 | 0.88 |
| CaO | 0.27 | 0.31 | 0.38 | 0.41 | 0.49 | 0.42 | 0.15 | 0.16 | 18.80 | 1.18 | 4.80 | 0.55 | 0.42 | 0.27 |
| Na ₂ O | 0.97 | 0.84 | 1.02 | 0.49 | 0.60 | 0.74 | 0.93 | 0.92 | 0.83 | 0.53 | 0.94 | 1.02 | 0.14 | 1.10 |
| K ₂ O | 0.84 | 0.63 | 1.04 | 0.49 | 0.55 | 0.95 | 0.11 | 0.08 | 0.14 | 0.02 | 0.14 | 0.20 | 0.23 | 0.34 |
| P ₂ O ₅ | 0.14 | 0.12 | 0.14 | 0.07 | 0.14 | 0.45 | 0.08 | 0.07 | 0.03 | 0.03 | 0.05 | 0.15 | 0.07 | 0.11 |
| Cl | 0.01 | 0.01 | 0.01 | 0.08 | 0.08 | 0.10 | 0.01 | 0.01 | 0.24 | 0.47 | 0.95 | 1.35 | 2.10 | 0.01 |
| SO ₃ | 0.01 | 0.01 | 0.01 | 0.06 | 0.14 | 0.30 | 0.01 | 0.01 | 0.11 | 0.65 | 4.75 | 0.17 | 0.10 | 0.01 |
| L.O.I | 1.71 | 1.38 | 2.45 | 13.04 | 13.60 | 13.18 | 2.67 | 1.13 | 21.45 | 12.96 | 12.18 | 10.05 | 10.95 | 3.02 |
| Trace elements in ppm | | | | | | | | | | | | | | |
| V | 989 | 391 | 840 | 229 | 219 | 273 | 408 | 346 | 110 | 110 | 121 | 333 | 686 | 434 |
| Cr | 1384 | 783 | 981 | 149 | 134 | 303 | 1689 | 523 | 362 | 253 | 215 | 177 | 747 | 251 |
| Co | 238 | 231 | 311 | 68 | 283 | 347 | 254 | 249 | 58 | 5 | 38 | 85 | 136 | 200 |
| Ni) | 46 | 41 | 1271 | 140 | 274 | 190 | 70 | 78 | 186 | 40 | 35 | 76 | 123 | 363.7 |
| Cu | 120 | 105 | 116 | 1537 | 3170 | 4178 | 146 | 41 | 28 | 189 | 1 | 2 | 1 | 1 |
| Zn | 1904 | 307 | 519 | 1751 | 2051 | 1854 | 203 | 330 | 1962 | 229 | 544 | 321 | 975 | 1751 |
| Rb | 15 | 4 | 15 | 11 | 12 | 10 | 2 | 14 | 17 | 7 | 10 | 0 | 13 | 16 |
| Sr | 1363 | 57 | 78 | 522 | 672 | 1350 | 64 | 64 | 2295 | 101 | 143 | 0 | 311 | 522 |
| Y | 28 | 30 | 25 | 39 | 55 | 140 | 10 | 9 | 15 | 13 | 10 | 0 | 14 | 24 |
| Nb | 8 | 8 | 7 | 1 | 1 | 3 | 1 | 10 | 3 | 1 | 1 | 0 | 1 | 5 |
| Ba | 127 | 166 | 166 | 2500 | 2500 | 2500 | 261 | 70 | 16 | 2241 | 1651 | 2500 | 185 | 59 |
| La | 80 | 50 | 58 | 46 | 68 | 101 | 39 | 23 | 11 | 25 | 19 | 0 | 31 | 46 |
| Pb | 233 | 19 | 23 | 86 | 237 | 235 | 28 | 35 | 74 | 29 | 72 | 95 | 174 | 86 |
| Zr | 196 | 83 | 106 | 93 | 71 | 280 | 27 | 27 | 253 | 31 | 13 | 0 | 42 | 56 |
| Elements ratios | | | | | | | | | | | | | | |
| MnO/F e ₂ O ₃ | 0.00 | 0.00 | 0.01 | 80.9 | 38.04 | 14.26 | 0.01 | 0.00 | 3.15 | 47.12 | 1.57 | 0.61 | 0.50 | 0.07 |
| Co/Ni | 5.17 | 5.63 | 0.24 | 0.49 | 1.03 | 1.83 | 3.63 | 3.19 | 0.31 | 0.13 | 1.09 | 1.12 | 1.11 | 0.55 |
| Co/Zn | 0.13 | 0.75 | 0.60 | 0.04 | 0.14 | 0.19 | 1.25 | 0.75 | 0.03 | 0.02 | 0.07 | 0.26 | 0.14 | 0.11 |

SiO₂ shows a positive correlation coefficient with Fe₂O₃ ($r= 0.82$) and negatively correlated with MnO ($r=-0.73$) which attributed to the presence of detrital quartz grains in the iron ores rather than manganese ores (Saad et al., 1994). The positive correlation coefficients among Co, Ni, Cu, Pb, Zn where Co-Ni ($r= 0.66$), Co-Cu ($r=0.81$), Co-Zn ($r= 0.62$), Co-Pb ($r= 0.89$), Ni-Zn ($r=0.80$), Cu-Zn ($r= 0.57$), Cu-Pb ($r= 0.80$) Zn-Pb ($r= 0.51$) may indicate their formation from hydrothermal solutions. The negative correlation between MnO with both MgO and CaO ($r= -0.61$ and -0.14 respectively) may reflect the replacement of carbonate minerals by manganese oxides. The positive correlation coefficients between SiO₂-TiO₂ ($r= 0.90$), SiO₂-V ($r= 0.57$), Al₂O₃-K₂O ($r=0.83$), Al₂O₃-P₂O₅ ($r=0.93$) and K₂O-P₂O₅ ($r=0.87$) may reflect the contribution of SiO₂, TiO₂, V, Al₂O₃, K₂O and P₂O₅ to mineralization where these elements are abundantly founded in sedimentary formations.

5.3. Major and Trace Elements Geochemistry

The major and trace elements contents and ratios in the Mn-rich ore (type 1) and Fe-Mn rich ore (type 2) are used herein to compare between the manganese ore at Um Bogma area and some worldwide manganese deposits depicted in table (3). Also due to the adsorption capacity of manganese and iron oxides for some elements such as Ba, Cu, Ni, Co, Pb, Sr, V, and Zn, several discrimination diagrams based on specific trace elements present in manganese oxides have been proposed to discriminate between the different genetic types of manganese ore (i.e., sedimentary, hydrothermal and hydrogenous) where such elements are frequently found in hydrothermal manganese-rich systems (Nicholson 1992a). In manganese ores, Cu, Co and Ni contents is an important indicator to recognize their origin. In the hydrothermal deposits, these elements are more abundant than pelagic deposits.

The relationships between sodium and magnesium oxides deposited in the fresh water, shallow-marine and marine environments (Nicholson, 1988) are given in Na-Mg discrimination diagram (Fig.5). In this diagram, the Um Bogma manganese-iron ore samples are mainly plotted in the area of shallow marine depositional environment except five sample plots on the fresh water environment. The lacustrine ferromanganese precipitates display low Na_2O and K_2O but a high $\text{CaO}/(\text{CaO} + \text{MgO})$ ratio (> 0.70) similar to the world average river water (Dasgupta et al., 1999). In contrast, diagenetically mature marine ferromanganese precipitates and nodules show a lower $\text{CaO}/(\text{CaO} + \text{MgO})$ ratio (< 0.60) in general, and variable Na_2O and K_2O . Consequently they used the Na_2O - CaO - MgO ternary diagram to distinguish between the ferromanganese deposits in marine and lacustrine environment. Plotting the data of Um Bogma Fe-Mn samples on the Na_2O - CaO - MgO diagram reveal that all of the Fe-rich ore and most of the Mn-rich ore are fall in the marine field (Figure 6).

Mn/Fe ratios in hydrothermal deposits are higher than 10 or lower than 0.1, but in hydrogenous deposits, it is about 1 (Rona, 1978). Higher amounts of Mn/Fe ratio or lower amounts of it is indicator of intense differentiation and segregation of these two elements in sedimentary environments and therefore is indicator of hydrothermal deposits. The Mn/Fe ratios for Mn-rich samples from the study area change in a wide interval (0.5 to 80.94). Such range indicates that the mineralization is not hydrogenetic but could be a hydrothermal type. The average Mn/Fe ratio in Mn-rich samples in the study area is 23.27 similar to Mn/Fe ratio in hydrothermal deposits at Baby Bare at the Northeast Pacific Ocean (Table 3).

Table 2: Pearson correlation coefficients between major oxides and trace elements of Um Bogma Mn-Fe ores.

| | <i>SiO₂</i> | <i>TiO₂</i> | <i>Al₂O₃</i> | <i>Fe₂O₃</i> | <i>MnO</i> | <i>MgO</i> | <i>CaO</i> | <i>Na₂O</i> | <i>K₂O</i> | <i>P₂O₅</i> | <i>V</i> | <i>Co</i> | <i>Ni</i> | <i>Cu</i> | <i>Zn</i> | <i>Rb</i> | <i>Sr</i> | <i>Ba</i> | <i>Pb</i> | <i>Zr</i> |
|------------------------------------|------------------------|------------------------|------------------------------------|------------------------------------|------------|------------|------------|------------------------|-----------------------|-----------------------------------|----------|-----------|-----------|-----------|-----------|-----------|-----------|-----------|-----------|-----------|
| <i>SiO₂</i> | 1 | | | | | | | | | | | | | | | | | | | |
| <i>TiO₂</i> | .900 | 1 | | | | | | | | | | | | | | | | | | |
| <i>Al₂O₃</i> | .07 | .33 | 1 | | | | | | | | | | | | | | | | | |
| <i>Fe₂O₃</i> | .82 | .53 | -.38 | 1 | | | | | | | | | | | | | | | | |
| <i>MnO</i> | -.73 | -.46 | .40 | -.94 | 1 | | | | | | | | | | | | | | | |
| <i>MgO</i> | .05 | -.06 | -.47 | .33 | -.61 | 1 | | | | | | | | | | | | | | |
| <i>CaO</i> | -.31 | -.22 | -.23 | -.18 | -.14 | .85 | 1 | | | | | | | | | | | | | |
| <i>Na₂O</i> | .45 | .57 | -.16 | .35 | -.40 | .31 | .21 | 1 | | | | | | | | | | | | |
| <i>K₂O</i> | .16 | .42 | .83 | -.27 | .36 | -.58 | -.35 | -.05 | 1 | | | | | | | | | | | |
| <i>P₂O₅</i> | .36 | .62 | .93 | -.14 | .19 | -.49 | -.33 | .13 | .87 | 1 | | | | | | | | | | |
| <i>V</i> | 0.57 | 0.29 | 0.06 | 0.68 | -0.57 | -0.05 | -.043 | -0.36 | 0.10 | 0.12 | 1 | | | | | | | | | |
| <i>Cr</i> | 0.18 | -0.07 | 0.07 | 0.33 | -0.41 | 0.28 | 0.11 | -0.58 | -.016 | -0.08 | .70 | | | | | | | | | |
| <i>Co</i> | 0.38 | 0.53 | 0.76 | 0.00 | 0.08 | -0.42 | -.034 | 0.02 | 0.87 | 0.81 | .29 | 1 | | | | | | | | |
| <i>Ni</i> | 0.47 | 0.52 | 0.09 | 0.31 | -0.26 | 0.03 | -.003 | 0.24 | 0.46 | 0.24 | .26 | .66 | 1 | | | | | | | |
| <i>Cu</i> | -0.14 | 0.17 | 0.85 | -0.56 | 0.63 | -0.64 | -.029 | -0.15 | 0.92 | 0.79 | -.14 | .81 | .32 | 1 | | | | | | |
| <i>Zn</i> | 0.00 | 0.20 | 0.31 | -0.18 | 0.13 | 0.02 | 0.24 | -0.01 | 0.64 | 0.32 | .00 | .62 | .80 | .57 | 1 | | | | | |
| <i>Rb</i> | 0.03 | -0.01 | -.013 | 0.07 | -0.18 | 0.35 | 0.43 | -0.12 | 0.11 | -0.17 | .10 | .22 | .63 | .03 | .72 | 1 | | | | |
| <i>Sr</i> | -0.13 | 0.12 | 0.30 | -0.31 | 0.06 | 0.48 | 0.77 | 0.09 | 0.29 | 0.23 | -.27 | .26 | .37 | .28 | .70 | .59 | 1 | | | |
| <i>Ba</i> | -0.37 | -0.15 | 0.42 | -0.60 | 0.75 | -0.74 | -.049 | -0.03 | 0.38 | 0.39 | .42 | .14 | -.35 | .56 | -.19 | -.70 | -.35 | 1 | | |
| <i>Pb</i> | 0.07 | 0.16 | 0.78 | -0.15 | 0.21 | -0.41 | -.031 | -0.30 | 0.79 | 0.69 | .36 | .89 | .40 | .80 | .51 | .13 | .20 | .21 | 1 | |
| <i>Zr</i> | -0.05 | 0.27 | 0.61 | -0.41 | 0.23 | 0.15 | 0.51 | 0.02 | 0.56 | 0.54 | -.23 | .44 | .30 | .53 | .67 | .43 | .91 | -.11 | .36 | 1 |

Table 3: Comparison between major and trace element contents of various worldwide types of manganese deposits with Mn-rich deposits (9 samples) at Um Bogma area. The major and trace elements contents of worldwide Mn-Fe ore are collected from Oksuz (2010).

| number of samples | 22 | 9 | 14 | 7 | 13 | 20 | 9 |
|------------------------------------|--------------------------|-----------------------------------|--------------|---------------|----------------------|---------------------|------------------------|
| regions | Hazara Pakistan | Baby Bare Northeast pacific ocean | Wakasa Japan | Uluken Turkey | Binkilic Turkey | Eymir Turkey | Um Bogma, Sinai, Egypt |
| origins | Hydrothermal-hydrogenous | Hydrothermal | Hydrothermal | Sedimentary | Sedimentary/diagenet | Volcano-sedimentary | this study |
| SiO ₂ (%) | 9.41 | 2.02 | 58.16 | 13.68 | 10.65 | 16.04 | 1.81 |
| TiO ₂ (%) | 0.84 | 0.04 | 0.04 | 0.1 | 0.02 | 0.02 | 0.05 |
| Al ₂ O ₃ (%) | 12.53 | 0.27 | 0.55 | 2.49 | 2.85 | 0.73 | 0.93 |
| Fe ₂ O ₃ (%) | 20.33 | 2.30 | 0.92 | 3.72 | 2.46 | 0.26 | 19.51 |
| MnO (%) | 33.78 | 48.52 | 32.5 | 63.78 | 33.39 | 69.91 | 57.26 |
| MgO (%) | 0.59 | 1.58 | 0.19 | 1.99 | 1.27 | 0.59 | 0.71 |
| CaO (%) | 6.43 | 0.97 | 4.15 | 4.05 | 18.96 | 2.4 | 3.38 |
| Na ₂ O (%) | 0.07 | 0.64 | 0.04 | 0.24 | 0.39 | 0.01 | 0.66 |
| K ₂ O (%) | 0.88 | 0.22 | 0.1 | 0.05 | 0.56 | 0.05 | 0.34 |
| P ₂ O ₅ (%) | 3.73 | 0.04 | 0.1 | 0.18 | 0.31 | 0.07 | 0.12 |
| Ba (ppm) | 6304 | 7091.67 | 13.79 | 427 | 6892 | 2364.7 | 1762 |
| V (ppm) | 573 | 172.33 | 258 | (-) | 106 | 132 | 260 |
| Cr (ppm) | 247 | 8.89 | 10 | (-) | 26 | (-) | 293 |
| Co (ppm) | 404 | 135.33 | 2 | 13 | 59 | 103.5 | 127 |
| Ni (ppm) | 305 | 300.67 | 28 | 10 | 167 | 67.35 | 133 |
| Cu (ppm) | 375 | 226 | 50 | 56 | 26 | 80.5 | 1138 |
| Zn (ppm) | 580 | 123.22 | 26 | 70 | 49 | 62.45 | 1211 |
| Pb (ppm) | 2357 | (-) | 112 | 65 | (-) | 9.33 | 125 |
| Rb (ppm) | 24 | 14.22 | 2 | (-) | (-) | 0.77 | 10 |
| Sr (ppm) | (-) | 877.44 | 85 | 185 | 2100 | 116.47 | 674 |
| Y (ppm) | (-) | 10 | 5 | (-) | 15 | 8.45 | 36 |
| Nb (ppm) | (-) | 1.5 | 3 | (-) | (-) | 0.15 | 1 |
| Zr (ppm) | (-) | 9.22 | 12 | (-) | 32 | 8.46 | 98 |
| Co/Ni | 1.32 | 0.45 | 0.07 | 1.3 | 0.35 | 1.54 | 0.88 |
| Co/Zn | 0.7 | 1.1 | 0.08 | 0.19 | 1.2 | 2.24 | 0.11 |
| Mn/Fe | 2.16 | 26.89 | 39 | 18.98 | 15.03 | 880.33 | 23.27 |

Al and Ti display similar behavior during the mineralization (Sugisaki, 1984 and Roy et al., 1990). Therefore, Al and Ti contents could also be used to evaluate the origin of mineralization. These two elements are abundantly found in sedimentary formations. High Al and Ti contents may indicate the sedimentary contribution to mineralization (Bonatti et al., 1972; Crerar et al., 1982; Roy et al., 1990 and Nicholson, 1992a). For sedimentary and diagenetic sedimentary Fe-Mn deposits in Table (3), the average Al and Ti concentrations are taken as 2.49-2.85% and 0.02-0.1%, respectively. The Al concentrations in the Mn-rich deposits in the study samples range between 0.26 to 3.16 wt % (average is 0.93 wt %) however, Ti concentrations range between 0.02 to 0.13 wt % (average is 0.05 wt %). These values are similar to hydrothermal deposits at Baby Bare at the Northwest Pacific Ocean (Table 3).

Cu, Zn, Pb and Ni are highly concentrated in Mn-rich ore at the study area (Table 2). They have average concentrations of 1138ppm for Cu, 1211ppm for Zn, 125ppm for Pb and 133ppm for Ni similar to those found in hydrothermal deposits at Baby Bare at the Northeast Pacific Ocean (Table 3). The higher concentrations of Cu, Pb and Zn are considered to be diagnostics of hydrothermal manganese deposits (Zantop, 1981; Nicholson, 1988).

The silica contents in hydrothermal manganese deposits are a matter of argument. The hydrothermal manganese deposits are commonly occur in close association with the ferruginous silica gel formed by submarine effusive processes and metal discharge into marine sediments and consequently, the hydrothermal manganese deposits are normally rich in their silica contents (Roy, 1992). In contrast, the association of the high contents of SiO₂ with the Fe-rich ore is attributed to the precipitation of Fe and Si first followed by Mn on the uppermost (most diluted) part of the flow forming zonal deposits with ferruginous-siliceous rocks at the base and manganese rocks at the periphery (Krauskopf, 1957; Hem, 1972 and Maynard, 1983). In the

study area, the Mn-rich ore samples contain low SiO_2 values (range between 1.07 to 2.90 wt %), conversely, the Fe-rich ore samples are rich in SiO_2 (8.6 to 10.10 wt %). In the Si-Al discrimination diagram of Choi and Harriya (1992) which distinguishes between hydrothermal and hydrogenous manganese oxides, the data from the Um Bogma manganese-iron oxides plot in the field characteristic of a hydrogenous origin (Figure 7). On the other hand, many manganese ore in the world have low concentration of silica as those in Baby Bare Northeast Pacific Ocean (Table 3). Plotting the data of the present study on the Fe-Si \times 2-Mn ternary diagram of Toth (1980) which distinguishes between the hydrothermal and diagenetic sources of manganese deposits reveal the hydrothermal origin for Um Bogma Mn-rich ore samples (Figure 8).

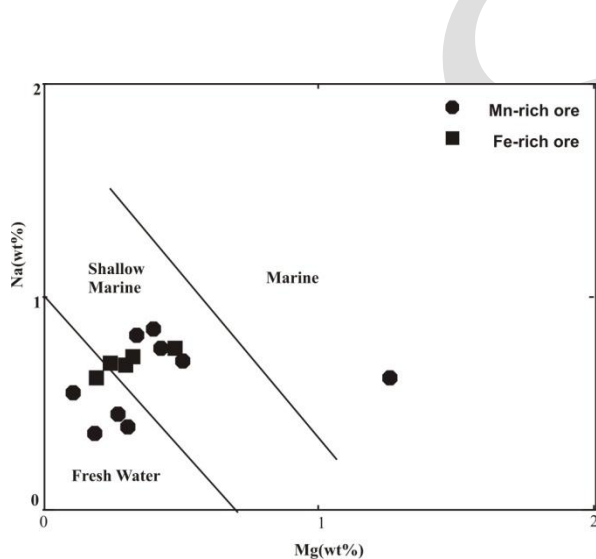


Figure 5: Um Bogma iron-manganese ore samples plotted on Mg-Na discrimination diagram of Nicholson (1988).

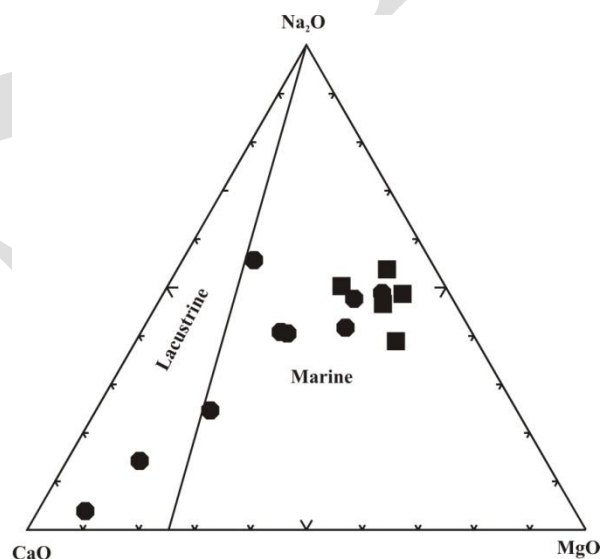


Figure 6: Um Bogma iron-manganese ore samples plotted on CaO- Na_2O -MgO discrimination diagram of Dasgupta et al. (1999).

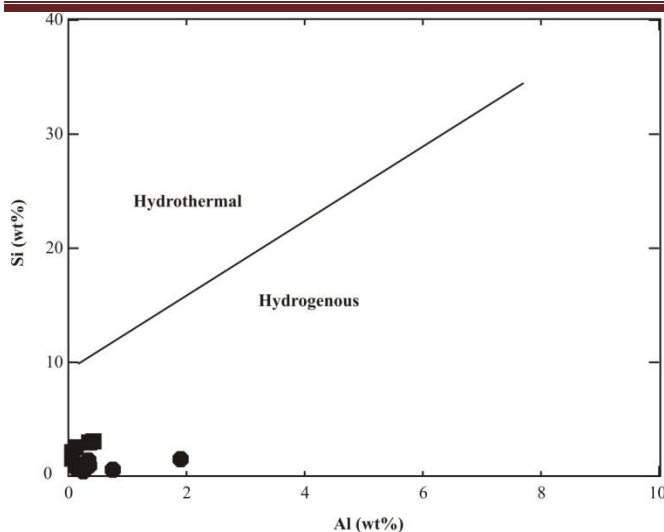


Figure 7: Al-Si discrimination diagram for the Um Bogma samples (after Choi and Hariya 1992).

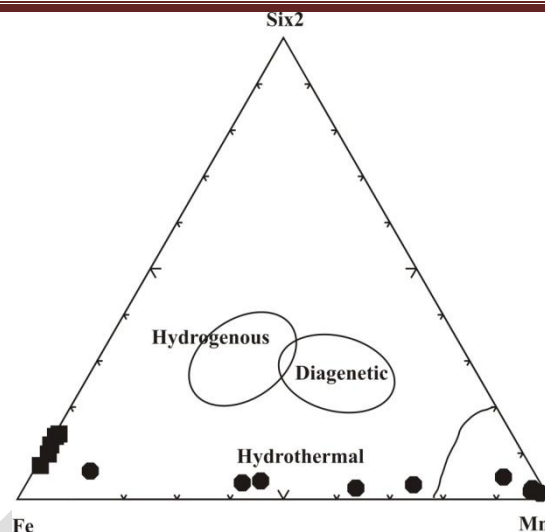


Figure 8: Fe-Si×2-Mn discrimination diagram for the Um Bogma samples (after Toth, 1980).

Toth (1980) used the Co/Zn ratio to differentiate between hydrothermal and hydrogenous type deposits where the Co/Zn ratio of 0.15 is indicative of hydrothermal type deposit and a ratio of 2.5 indicates hydrogenous type deposits. The Co/Zn ratios of Um Bogma Mn-Fe deposits range between 0.03 and 0.26 (average 0.11) more or less around the Co/Zn ratio for hydrothermal manganese deposits given by Toth (1980) and the hydrothermal deposits at Wakasa Japan (Table 3). Co, Ni and Zn elements in manganese formations are absorbed on Mn oxide surface (Toth, 1980). High cobalt concentrations are indicative of marine environments as pointed out in the discrimination diagram between supergene and hydrothermal deposits of Nicholson (1992b). In this respect, most Um Bogma samples plotted in the hydrothermal field (Figure 9).

Mn-Fe-(Co+Ni+Cu)×10 discrimination diagram was used to discriminate between hypogenetic and exhalative hydrothermal iron-manganese deposits (Bonatti et al.; 1972, Crerar

et al.; 1982 and Nicholson; 1992a). The distribution of Fe-Mn ore samples of Um Bogma area are shown in figure (10). In this respect all samples are plotted in hydrothermal and field.

Monnin et al. (2001) mentioned that hydrothermal solutions are more enriched in Ba compared to seawater since they are affected from volcanic activity and sedimentation. Ba concentrations in the Mn-rich-types at Um Bogma manganese deposit are in the range of 2241 to 2500ppm (average 2435ppm) similar to volcano-sedimentary manganese deposits at Eymir, Turkey (Table 3)

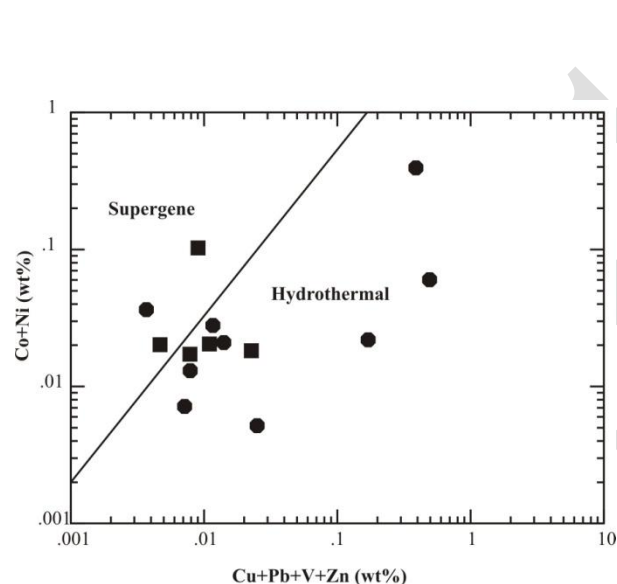


Figure 9: Co + Ni versus Cu + Pb + V + Zn discrimination diagram for the Um Bogma samples (after Nicholson, 1992 b).

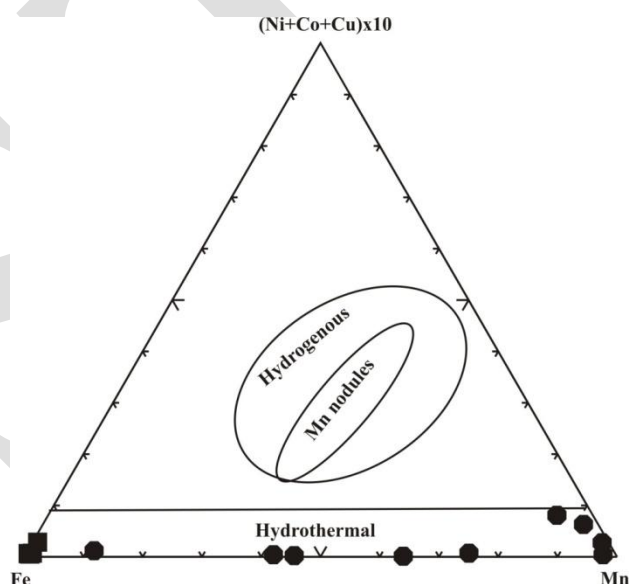


Figure 10: Mn-Fe-(Co+Ni+Cu) \times 10 discrimination diagram for the Um Bogma samples after Bonatti et al.; 1972, and Crerar et al.; 1989)

6. CONCLUSIONS

Manganese-iron ores are located within the Paleozoic rocks at Um Bogma area, west central Sinai. The mineralization does not confined to specific horizons in the Paleozoic rocks but it is reported as spots and encrustation in the sandstones and shales of the Lower sandstone Series. The main manganese-iron ore are recorded in many morphological shapes as lenticular

bodies, sheets, encrustation and filling the fractures in the Um Bogma Formation especially in the Lower dolomite Member and the marly dolomite Member. They are chemically classified into three types depending on their contents of manganese and iron oxides and on the MnO/Fe₂O₃ ratios. Type 1 is the Mn-rich ore has high contents of MnO, Cu, Zn, Pb, Co, Ni, Ba, Zr and low contents of low Fe₂O₃, SiO₂, TiO₂, V, Sr and Nb. Type 2 is Mn-Fe rich ore has more or less equal contents of both MnO and Fe₂O₃. This type is relatively has high contents of SO₃, Zn, Sr and low contents of Al₂O₃, TiO₂, Co, Ni and Cu. Type 3 is Fe- rich ore has high contents of Fe₂O₃, SiO₂, TiO₂, V, Cr, Co, Ni, Nb and low contents of MnO, Al₂O₃, SO₃, Cu Sr, Ba, Pb and Zr.

Based on the results of major and trace element data, the manganese-rich ores in the study area was probably formed from hydrothermal solutions. For instance, the high Mn/Fe ratios (average 23.27) indicate the mineralization could be a hydrothermal type (Rona, 1978). The low Co/Zn ratios (average 0.11) are around the Co/Zn ratio for hydrothermal manganese deposits (Toth, 1980). The high concentration of Cu, Pb, Zn, Ba, and Ni in addition to the good correlation among them may indicate their formation from hydrothermal solutions. The negative correlation coefficients between MnO with both MgO and CaO may reflect the replacement of carbonate minerals by manganese oxides. The positive correlation coefficients between SiO₂, TiO₂, V, Al₂O₃, K₂O and P₂O₅ can be attributed to the mixing of detrital materials during precipitation. The Fe-Mn ores at Um Bogma area also have a hydrothermal character based on the discrimination diagrams of Nicholson (1992b), Toth, (1980) and Bonatti et al. (1972).

REFERENCES

- Ashami, A.S. (2003): Structural and lithologic controls of uranium and copper mineralization in Um Bogma environs, southwestern Sinai, Egypt, PhD Thesis, Mansoura Univ., Egypt, 134p.
- Attia, M.I. (1956): Manganese deposits of Egypt. 20th Intern. Geol. Cong. Mexico. Symp. Sopyacim. Mang. T. II: (Africa), pp. 143-171.
- Ball, J. (1916): The geography and geology of west central Sinai: Survey Dept., Cairo, pp. 186-204.
- Barron, T. (1907): The topography and geology of the peninsula of Sinai (Western portion): Survey Dept., Cairo, 241p.
- Basta. E.Z. and Saleeb, W.S. (1971): Mineralogy of the manganese ores of Elba area, South Eastern Desert. Jour. of Geology. Vol. XV. No. 1, pp. 29-48.
- Bonatti, E., Kraemer, T., Rhydell, H. (1972): Classification and genesis of submarine iron-manganese deposit. In: Horn, D.R. (Ed.), Ferromanganese Deposits on the Ocean Floor. Earth and Planet Sci. Let., pp. 229-238.
- Choi, J. H. and Hariya, Y. (1992): Geochemistry and depositional environment of Mn oxide deposits in the Tokoro Belt, Northeastern Hokkaido, Japan. Econ. Geol. 87, pp. 1265–1274.
- Crerar, D.A., Namson, J., Chyi, M.S., Williams, L. and Feigenson, M.D. (1982): Manganiferous cherts of the Franciscan assemblage: I. General geology, ancient and modern analogues, and implications for hydrothermal convection at oceanic spreading centers,” Econ. Geol. 77, pp. 519–540.
- Dasgupta, H.C., Sambasiva Rao, V.V., Krishna, C. (1999): Geology, geochemistry and genesis of the freshwater, Precambrian manganese deposit of the iron ore group from Noamundi basin, Eastern India. Indian J. Geol. 71, pp. 247–264.
- El Agami, N. L. (1996): Geology and radioactivity studies on the Paleozoic rock units in the Sinai Peninsula, Egypt, Ph.D. Thesis, Fac. of Science, Mansoura Univ., Egypt, 302 p.
- El Fiky A. M. (1988): Sedimentologic and radiometric studies on some Paleozoic sediments in west central Sinai, Egypt. M.Sc. Thesis, Suez Canal Univ., Egypt, 204 p.
- El Sharkawi, M.A., El Aref, M.M. and Abdel Motelib, A. (1990): Manganese deposits in a Carboniferous paleokarst profile, Um Bogma region, west-central Sinai, Egypt: Mineral. Deposita, vol. 25, pp. 34-43.

- El Shazly, E.M., Shukri, N.N. and Saleeb, G.S., (1963): Geological studies of Oleikat, Marahil and Um Sakran manganese-iron deposits, west central Sinai: J. Geol., U.A.R. vol. 7. (1), pp. 1-27.
- Gill, D. and Ford, S.O. (1956): Manganiferous iron ore deposits of the Um Bogma district, Sinai, Egypt: International Geologic Congress, Mexico, Symp. Sabre Yecimientos de manganese, vol. 2, pp. 173-177.
- Hein J R, Kochinsky A, Halbach P, Manheim F T, Bau M, Kang J K, Lubick N. (1997): Iron and manganese oxide mineralization in the Pacific. In: Nicholson K, Hein J R, Buhn B, Dasgupta S. (Eds.). Manganese Mineralization: Geochemistry and Mineralogy of Terrestrial and Marine Deposits, Geol. Soc. Lond. Spec. Publ., 119: 123p.
- Hein J R, Yeh H W, Gunn S H, Gibbs A E, Wang C H. (1994): Composition and origin of hydrothermal ironstones from central Pacific seamounts. Geochim. Cosmochim. Acta, 58, 179p.
- Hein, J R, Gibbs, A E., Clague, D., Torresan, M. (1996): Hydrothermal mineralization along submarine rift zones, Hawaii. Mar. Georesour. Geotechnol., 14: 177p.
- Hem, J.D. (1972): Chemical factors that influence the availability of iron and manganese in aqueous systems, Bull. Geol. Soc. Am., 1972, vol. 83, pp. 443–450.
- Hussein, H.A., Anwar, Y.M. and El-Sokkary, A.A. (1971): Radiogeologic studies of some carboniferous rocks of west central Sinai, U.A.R. J.Geol., 15, pp. 119- 127.
- Ingram B L, Hein J R, Farmer G L. (1990): Age determinations and growth rates of Pacific ferromanganese deposits using strontium isotopes. Geochim. Cosmochim. Acta, 54: 1709p.
- Issawi, B. and Jux, U., (1982): Contribution to the stratigraphy of the Paleozoic rocks in Egypt. M.Sc. Thesis, Cairo Univ., Egypt, 249p.
- Klinkhammer G P, Heggie D T, Graham D W. (1982): Metal diagenesis in oxic marine sediments. Earth Planet. Sci. Lett., 61, 211p.
- Kora, M. (1984): The Paleozoic outcrops of Um Bogma area, Sinai: Ph.D. thesis, Monsoura Univ., Egypt 280 p.
- Kora, M. and Jux, Y., (1986): On the early Carboniferous macrofauna from Um Bogma Formation, Sinai, N.Jb. Geol. Palaont. Mh., H.2, Stuttgart, pp. 85-98.
- Kora, M. (1989): Lower Carboniferous (Visean) fauna from Wadi Budra, west-central Sinai, Egypt. Monatshefte Neues Jahrbuch Geologie Palaontologie (9), pp. 523-538.

- Kora, M., El Shahat, A. and Abu Shabana (1994): Lithostratigraphy of the manganese bearing Um Bogma Formation, West Central Sinai, Egypt. *J. Afr. Earth. Sci.*, 18 (2), pp. 15-162.
- Kotchin, G.G. and Bassyoni, F.A. (1968): Studies on some mineral deposits of Egypt. *Geol. Surv. Egypt. Internal Report*.
- Krauskopf, K.B. (1975): Separation of manganese from iron in sedimentary processes, *Geochim. Cosmochim. Acta*, vol. 12, pp. 61–84.
- Kuhn T, Bau M, Blum N, Halbach P. (1998): Origin of negative Ce anomalies in mixed hydrothermal-hydrogenetic Fe-Mn crusts from the Central Indian Ridge. *Earth Planet. Sci. Lett.*, pp. 163: 207.
- Manheim F T, Lane-Bostwick C M. (1988): Cobalt in ferromanganese crusts as a monitor of hydrothermal discharge on the Pacific seafloor. *Nature*, 335: 59p.
- Mart, J. and Sass, E. (1972): Geology and origin of the manganese ore of Um Bogma, Sinai: Reprint from *Economic Geology*, vol. 67, No.2, pp. 145-155.
- Maynard, J.B. (1983): *Geochemistry of Sedimentary Ore Deposits*, New-York, Heidelberg: Springer.
- Monnin C, Wheat C G., Dupre B, Elderfield H, Mottl M J. (2001): Barium geochemistry in sediment pore waters and formation waters of the oceanic crust on the eastern flank of the Juan de Fuca Ridge (ODP Leg 168). *Geochem. Geophys. Geosyst.*, 2: 1.
- Monsour, M.(1994): Sedimentology and radioactivity of Um Bogma Formation, West Central Sinai, Egypt M.Sc. Thesis, Faculty of science, Suez Canal Univ., 157 p.
- Nakhla, F.M. and Shehata, M.R.N., (1963): Mineralogy of some manganese-iron ores from west central Sinai, Egypt: *N-Jb Miner., Abh.* Vol. 99, N.3, pp. 277-294.
- Nicholson, K. (1988): An ancient manganese-iron deposits of fresh water origin, Islay, Argyllshire. *Scott J. Geol* 24 (2): pp. 175-187.
- Nicholson, K. (1992a): Genetic types of manganese oxide deposits in Scotland: Indicators of paleo ocean spreading rate and a Devonian geochemical mobility boundary. *Econ. Geol.* 87, pp. 1301–1309.
- Nicholson, K., (1992b): Contrasting mineralogical–geochemical signatures of manganese oxides: Guides to metallogenesis. *Econ. Geol.* 87, pp. 1253–1264.
- Oksuz N, (2011): Examination of Sarikaya (Yozgat-Tyrkey) iron mineralization with rare earth element (REE) method. *Journal of Rare Earths*, 28(1):143.

- Rona, P. A. (1978): Criteria for recognition of Hydrothermal Mineral Deposits in Oceanic crust. *Econ. Geol.* 73, pp. 135-160.
- Roy, S., Dasgupta, S. Mukhopadhyay, S. and Fukuoka, M. (1990): Atypical ferromanganese nodules from pelagic areas of the Central Indian Basin, Equatorial Indian Ocean. *Mar. Geol.* 84, pp. 339–349.
- Roy, S., (1992): Environments and processes of manganese deposition. *Econ. Geol.* 87, pp. 1218-1236.
- Saad, N., Zidan, B.I. and Khalil, K.I. (1994): Geochemistry and origin of the manganese deposits in the Urn Bogma region, west central Sinai, Egypt. *J. African Earth Sciences*, 1911-2 pp. 109-116.
- Saleeb-Roufaiel, G.S., Yanni, N.N. and Arner, K.M. (1987): Contribution to the study of manganese-iron deposits at Urn Bogma area, Sinai. Middle East Research Centre, Ain Shams University, Earth Sciences Series 1, pp. 98-107.
- Simmonds and Ghasemi (2007): Investigation of Manganese Mineralization in Idahlu and Jokandy, Southwest of Hashtrood, NW Iran. *BHM*, 152, Jg. Heft 8.
- Soliman, M.S. and Abu El Fetouh, M. A., (1969): Petrology of Carboniferous sandstones in west central Sinai: Reprint from *Journal of Geology of the United Arab Republic*, vol. 13 (2), pp. 61-143
- Sugisaki, R. (1984): Relation between Chemical Composition and Sedimentation Rate of Pacific Ocean Floor Sediments Deposited since the Middle Cretaceous: Basic Evidence for Chemical Constraints on Depositional Environments of Ancient Sediments. *J. Geol.* 92, pp. 235–259.
- Toth, J. R. (1980): Deposition of submarine crusts rich in manganese and iron. *Geological Society of America Bulletin*, 91, pp. 44.
- Weissbrod, T. (1981): The Paleozoic of Israel and adjacent countries (Lithostratigraphic study). Report M.P. 600/81 Min. Res. Div. Geol. Survey, Israel, 1981.
- Weissbrod, T. (1969): The Paleozoic outcrops in south Sinai and their correlation with those of southern Israel, in the Paleozoic of Israel and the adjacent countries: *Geol. Surv. Israel. Bull.* No. 47, pt, 2, 2, 32p.
- Zantop, H. (1981): Trace elements in volcanogenic manganese oxides and iron oxides: the San Francisco manganese deposit, Jalisco, Mexico. *Econ. Geol.* 76, pp. 545–555.